0026-895X/96/040838-08$3.00/0

MOLECULAR PHARMACOLOGY, 50:838–845 (1996).

Aza-bioisosteres of 9,10-anthracenedione: A Modulation of DNA Sequence Specificity

CLAUDIA SISSI, GIOVANNI CAPRANICO, ERNESTO MENTA and MANLIO PALUMBO

Department of Pharmaceutical Sciences, University of Padova, 35131 Padova, Italy (C.S., M.P.), Istituto Nazionale per lo Studio e la Cura dei Tumori, Oncologia Sperimentale B, 20133 Milano, Italy (G.C.), and Research Center, Boehringer Mannheim Italia, 20052 Monza, Italy (E.M.)

Received April 11, 1996; Accepted June 26, 1996

SUMMARY

The sequence specificity of DNA-binding by monoaza- and diaza-anthracenedione analogues of mitoxantrone (MX) has been investigated by DNase I footprinting and spectroscopic techniques. More than 100 sites cut by the enzyme were sequenced on three pBR 322 and simian virus 40 DNA restriction fragments. Different inhibition and stimulation effects were observed as a function of the structural properties of each drug. A gradual change was found from MX to monoaza derivatives and from these to diaza derivatives, corresponding to a broader distribution of drug-inhibited regions. In addition to almost all sites found with MX (38 of 44), 29 new inhibition sites were observed using the diaza compound BBR 2894. The sequence analyses in terms of base doublets or triplets confirm the preference of MX for alternating pyrimidine-purine sites, the most significant triplet sequences being (5′ to 3′) CTA, GCA, TAC, ACT, CAC and TTA. In addition to MX sites, BBR 2894 seemed to bind efficiently to pyrimidine-pyrimidine-pyrimidine or purine-pyrimidine-pyrimidine triplets containing CT or TC motifs. Differential cleavage plots essentially confirmed the above results. Spectrophotometric and chiroptical studies showed a decreased DNA-binding affinity and a modified geometry of intercalation when nitrogen replaces carbon in the anthraquinone ring. These results can be useful for understanding the substantially different biological responses exhibited by aza-substituted anthracenediones when compared with their non-substituted, pharmacologically relevant congeners.

In human cancer therapy, MX is probably the most effective compound among synthetic anthraquinone derivatives related to anthracycline antibiotics (1). Because of its wide-spectrum anticancer activity, MX is currently used in the treatment of numerous malignancies, such as leukemia, lymphomas, and ovarian and breast cancer (2).

The drug has a planar ring system that is able to intercalate into DNA and two positively charged side chains that strengthen the affinity for nucleic acids (3). These facts are believed to be related to the drug's mode of action and toxicity, because MX-induced cell death is invariably accompanied by DNA fragmentation. The latter can be accounted for by at least two main mechanisms: one, which is associated with protein, involves trapping of a protein (topoisomerase II)-DNA cleavable intermediate (4–6), whereas the other, a non-protein-associated mechanism, is related to redox cycling of the anthracenedione moiety, which produces damaging free-radical species (7, 8). In both cases, the distribution of damage along the DNA chain is not random but obeys well defined specificity criteria that are related to drug structure (9–12).

MX has been widely investigated in terms of specificity for DNA with the use of spectroscopic and footprinting techniques as well as theoretical calculations (3, 13–18). Although not all reports agree, MX seems to prefer intercalation at 5′-pyrimidine-purine-3′ steps. An additional element of discrimination seems to be located at the base preceding the pyrimidine, so that the drug recognizes triplets rather than pairs of bases, the most effective consensus sequences being (A/T)CA and (A/T)CG (15). A similar three-base recognition motif has been proposed for anthracyclines on both theoretical and experimental bases (19–21).

A large number of MX derivatives intended as more effective anticancer agents have been investigated during the last few years (22, 23). Although most of the modifications were located in the side chains, more recently, changes have been introduced into the anthracenedione moiety, too. In particular, the carbon-to-nitrogen isosteric substitution has received increasing attention and has led to the development of the aza-anthraquinone family, which exhibited a spectrum of biological activity distinct from that of MX (24–28). In fact, protein-associated DNA damage is dramatically decreased, whereas free-radical damage still seems to occur to a considerable extent (29, 30).

Differences in selective targeting of aza-anthraquinones onto DNA might play a major role among factors responsible for the distinct pharmacological behavior shown by otherwise

This work has been carried out with the financial support of Associazione Italiana per la Ricerca sul Cancro.

ABBREVIATIONS: MX, mitoxantrone; SV40, simian virus 40.

very similar compounds. An evaluation of sequence-specific binding of the new drugs to the nucleic acid represents, therefore, an essential step toward gaining a deeper insight into structure-activity relationships. We will present here an investigation on the DNA sequence preference of mono- and diaza-anthracenediones (Fig. 1), along with MX, using both spectroscopic and DNase I footprinting techniques.

Experimental Procedures

Materials. BBR 2778 [6,9-bis[(2-aminoethyl)amino]benzo[*g*]isoquinoline-5,10-dione], BBR 2378 [6,9-bis[(2-dimethylaminoethyl)-amino]benzo[*g*]isoquinoline-5,10-dione], BBR 2868 [6,9-bis[(2-aminoethyl)amino]benzo[*g*]isoquinoline-5,10-dione-2-oxide], BBR 2867 [6,9-bis[(2-dimethylaminoethyl)amino]benzo[*g*]isoquinoline-5,10-dione-2-oxide], BBR 2894 [6,9-bis[(2-aminoethyl)amino]benzo-[*g*]phtalazine-5,10-dione], and MX were synthesized according to Krapcho *et al.* (25, 26). Stock solutions (2 mM) were prepared in water and stored at −20°. These solutions were diluted to the appropriate concentration in the working buffer immediately before use.

DNase I, poly(dA-dT) and poly(dG-dC) were purchased from Sigma (St. Louis, MO) and used without further purification. pBR 322 and SV40 DNAs were purchased from Boehringer Mannheim (Mannheim, Germany).

DNA fragments. Three 5′-end-labeled DNA fragments were used: an *Acc*I-*Eco*RI fragment of pBR 322 DNA labeled at the *Acc*I site, a *Taq*I-*Eco*RI and a *Bam*HI-*Acc*I fragment of SV40 DNA labeled at the *Taq*I and *Bam*HI sites, respectively.

The DNA labeling procedure was essentially as previously described (10). Briefly, the DNA was first linearized with the appropriate restriction enzyme under the conditions recommended by the supplier. DNA was dephosphorylated with calf alkaline phosphatase (Boehringer Mannheim) and then labeled with [γ-^{32}P]ATP and T4 polynucleotide kinase. After phenol-chloroform extraction and ethanol precipitation, DNA was digested with the second restriction enzyme. The uniquely 5′-end-labeled DNA fragments were then separated by 1% agarose gel electrophoresis and electroelution. The fragments used allowed us to examine drug-DNA interaction from nucleotide −2520 to −2410 and from 4750 to 4855 in SV40 and from nucleotide 2250 to 2370 in pBR 322.

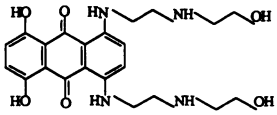

MITOXANTRONE

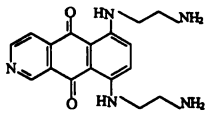

BBR 2778

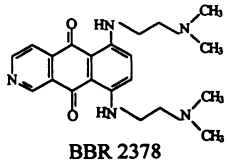

BBR 2378

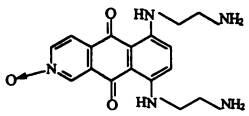

BBR 2868

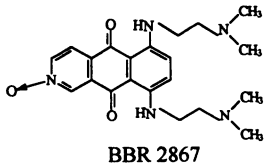

BBR 2867

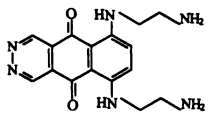

BBR 2894

Fig. 1. Molecular structure of the test anthracenedione derivatives.

DNase I footprinting. 20,000 cpm of 5′-labeled DNA was mixed with unlabeled DNA (final concentration, 20 μM) and scalar concentrations of the test drugs in DNase I buffer (40 mM Tris·HCl, pH 7.9, 10 mM NaCl, 6 mM $MgCl_2$, and 0.1 mM) $CaCl_2$. The mixture was incubated for 30 min at 30° and then cooled to 4°. At this temperature, DNase I was added (0.5 units in a final volume of 20 μl). The reaction was stopped at different times by cooling in ice and adding 10 μl of 60 mM EDTA and 60 μl of stop mixture (10 mM Tris·HCl, pH 8.0, 0.1 mM EDTA, 450 mM NaOAc, 2 μg/μl salmon sperm, 5 μg/μl yeast tRNA). After ethanol precipitation, the fragments were washed, dried, suspended in sequencing loading buffer (80% formamide, 10 mM NaOH, 1 mM EDTA, 0.1% xylene cyanol, 0.1% bromphenol blue), heated for 2 min at 90°, chilled in ice and loaded onto 8% denaturing polyacrylamide gel (19:1) in Tris/borate/EDTA buffer (89 mM Tris base, 89 mM boric acid, 2 mM Na_2EDTA). Gels were transferred to Whatman 3MM paper (Whatman, Maidstone, UK), dried under vacuum at 80°, and autoradiographed (Amersham Hyperfilm MP; Amersham, Arlington Heights, IL) at −70° with an intensifying screen (14). Autoradiographs were scanned on a Shimadzu dual wavelength chromato scanner CS-9930 and data recorded on a Shimadzu DR-2 apparatus (both from Shimadzu Europe GMBH, Duisburg, Germany).

For each phosphodiester bond, the fractional cleavage in presence or absence of the drugs was calculated as (area under the peak)/(total area). Comparison was carried out on lanes in which digestion was similar and not too extended to reduce the incidence of multiple cuts in any one strand. Data were reported as $[\ln(f_a)-\ln(f_c)]$ were f_a is the fractional cleavage at any bond in the presence of the drug and f_c is the fractional cleavage of the same bond in the control, so that positive values indicate enhanced cleavage whereas negative values represent ligand protected sites. Graphical representations were obtained plotting the average of $[\ln(f_a)-\ln(f_c)]$ at any bond with those of its two nearest neighbors (31).

DNA binding. The DNA binding properties of test compounds were investigated spectrophotometrically on a Perkin Elmer Lamba 5 Spectrophotometer (Norwalk, CT) in the drug absorption range. Titrations were carried out in EDTA/Tris/NaCl buffer (10 mM Tris, 1 mM EDTA, NaCl to the desired ionic strength, pH 7.0). In the ionic strength range 0.1–0.25 M, the presence of an isosbestic point during titration with DNA allowed an evaluation of the fractions of free and bound ligand. To avoid large systematic inaccuracies caused by to experimental errors in extinction coefficients, the range of analyzed bound drug fractions was 0.15–0.85. Data were evaluated according to the McGhee and Von Hippel method (32), which yields the intrinsic binding constant, K_i, and the exclusion parameter, n.

Chiroptical Studies

Circular and linear dichroism spectra were recorded on a Jasco 500A Spectropolarimeter interfaced with a Jasco 501N data processor (both from Jasco, Tokyo, Japan). Experimental data were analyzed on a Compaq MT 4/66 Personal Computer. Quartz cells that had 10-mm path-lengths were used, and 4–8 scans were accumulated for each measurement. Linear dichroism spectra were recorded on the same spectropolarimeter equipped with a cylindrical cell with 1-mm optical path-length. Orientation of DNA was achieved by rotating the inner cell wall at 900 rpm.

Results

DNase I Footprinting

DNase I footprinting experiments (33) were performed on three DNA restriction fragments from pBR 322 and SV40 in the presence or absence of the test drugs. As in the case of MX

(14), enzyme digestion at 37° showed no clear drug-induced modification of the cutting pattern. On the contrary, at 4° (Fig. 2), drugs interfere efficiently with DNase I cleavage, generating a footprinting pattern that is clearly distinctive when comparing the aza derivatives with the parent anthraquinone MX. Characteristic features of the footprinting pattern are designated in Fig. 2 (*arrows*). In fact, positions −2475 and −2496 in Fig. 2A represent strong stimulation sites for MX but not for the aza analogues, whereas around positions −2426 and −2442, aza compounds modify DNase I cleavage to a much larger extent than does MX. Further examples of clear-cut differences between MX and the other derivatives are indicated in Fig. 2B.

The effects of drug concentration and time of incubation upon cleavage were also evaluated. In general, to induce a significant modification of the DNase I cleavage pattern, a higher concentration of aza-anthraquinone derivatives was required in comparison with MX. This may be because of a reduced affinity of the new compounds for the DNA target. Increasing the incubation time leads to a loss of the protection/enhancement pattern, which is probably connected to the reversible nature of the drug-DNA binding process (34). This is particularly evident with the monoaza derivatives; a 5-min incubation is enough to lose the footprinting information (compare the appropriate *lanes a* and *b* in Fig. 2B).

The DNase I cleavage patterns presented in Fig. 2 allow an evaluation of template sites at which cleavage is inhibited or enhanced. Indeed, a modulation in the response is observed as a function of drug structure; MX and the diaza derivative are the most divergent, and all monoaza derivatives exhibit an intermediate behavior. Moreover, compounds that have the same ring system exhibit almost identical cleavage patterns, regardless of the side-chain structure. Hence, MX and BBR 2894 were chosen as the key representatives of two

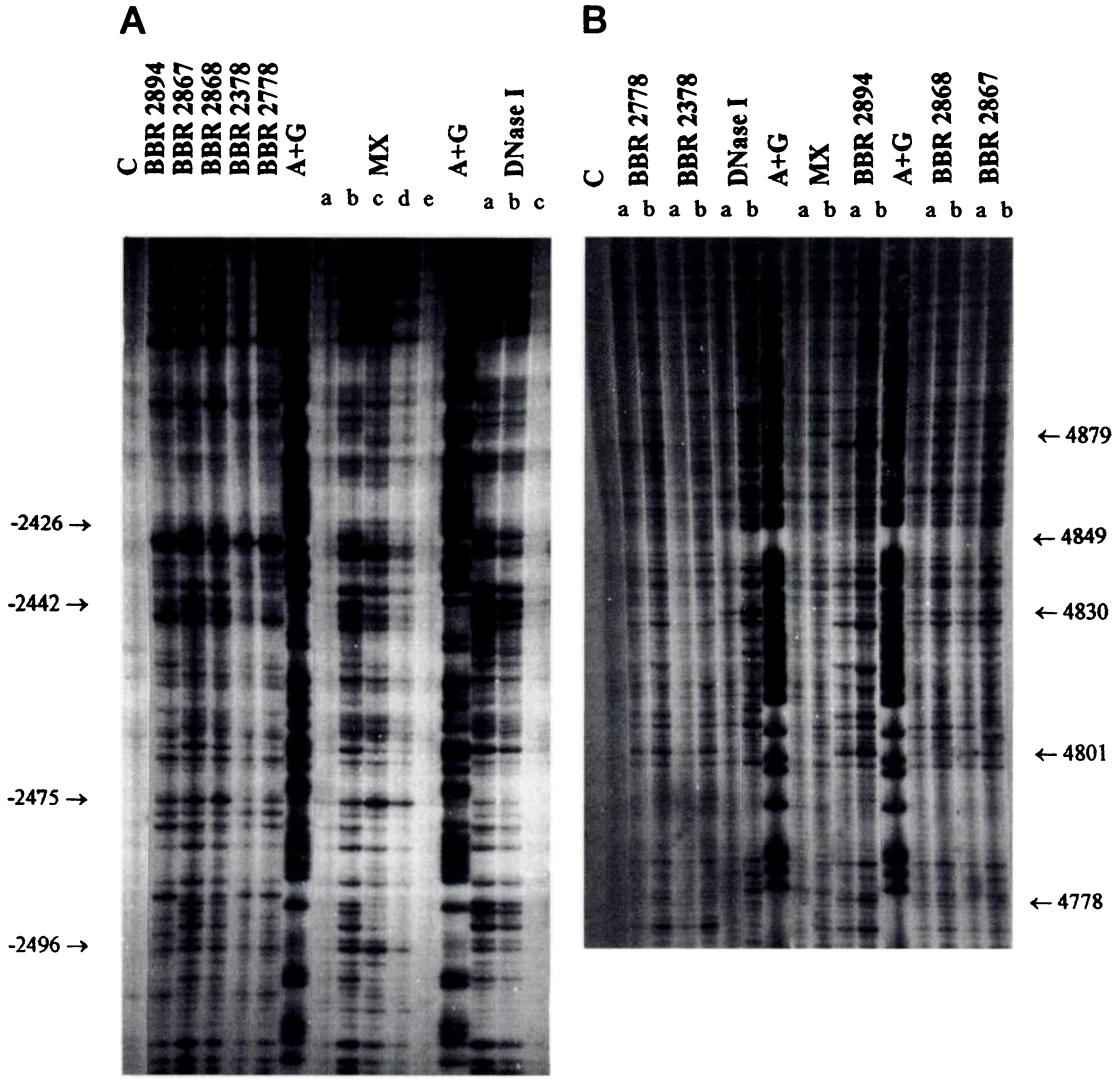

Fig. 2. Autoradiographs of DNase I footprinting of the test anthracenediones on restriction fragments that were 5′-end labeled with [γ-^{32}P]ATP. The products of DNase I digestion (2.5 units/ml) carried on at 4° were resolved on a 8% polyacrylamide gel containing 7 M urea. *Lane C*, labeled DNA incubated without drugs or enzyme; *lanes DNase I*, products of enzyme digestion in the absence of drugs; *lane A+G*, Maxam-Gilbert purine markers used for reference. *Arrows*, characteristic features of the footprinting pattern. A, SV40 (*Bam*HI-*Acc*I restriction fragment). The concentration of BBR derivatives is 10 μM and the incubation time is 1 min. The concentrations of MX are: *lane a*, 10 μM, 1-min incubation time; *lane b*, 1 μM, 1-min incubation time; *lanes c, d and e*, 5 μM, 5-min, 1-min, and 10-sec incubation times, respectively. *Lanes a, b, and c*, incubation times for DNase I alone, 5 min, 1 min, and 10 sec, respectively. B, SV 40 (*Taq*I-*Eco*RI restriction fragment). Drug concentration is 10 μM for aza derivatives and 5 μM for MX. *Lanes a and b*, 1- and 5-min incubation times, respectively.

TABLE 1

Modification of DNase I cutting induced by mitoxantrone and BBR 2894 on SV40 and pBR 322 fragments

Data are analyzed in terms of base doublets.

Sequence (5′→3′)	N[a]	DNase I[b]	MX		BBR 2894	
			I[c]	S[d]	I[c]	S[d]
A A	16	3	1	1	1	1
T T	26	9	2	1	8	0
A C	20	10	6	3	3	8
G T	16	6	5	1	4	2
A G	23	12	4	5	6	3
C T	23	13	7	4	12	2
A T	25	14	4	3	7	4
T A	20	3	3	2	2	2
T C	16	11	1	3	10	3
G A	13	1	0	0	0	1
T G	19	10	4	1	8	0
C A	35	5	1	2	1	0
C C	23	1	0	2	0	9
G G	9	1	0	0	0	2
C G	8	5	2	0	4	0
G C	22	4	4	1	2	5

[a] number of selected sequences in examined DNA fragments.
[b] number of selected sequences cut by DNase I.
[c] sites of drug inhibition of DNase I cutting.
[d] sites of drug stimulation of DNase I cutting.

TABLE 2

Modification of DNase I cutting induced by mitoxantrone and BBR 2894 on SV40 and pBR 322 fragments

Data are analyzed in terms of base triplets DNase I cuts occur between the bases in capital letters.

Sequence (5′→3′)	DNase I[a]	MX		BBR 2894	
		I[b]	S[c]	I[b]	S[c]
yYYn	26	8	8	23	15
nRRr	11	3	4	6	6
rYYn	8	2	2	7	0
nRRy	6	2	2	1	1
nYYy	16	4	6	14	15
rRRn	4	1	1	2	2
nYYr	18	6	4	16	0
yRRn	13	4	5	5	5
yYRn	12	7	1	9	2
nYRr	10	3	3	5	2
rYRn	11	3	4	6	0
nYRy	13	7	2	10	0
yRYn	28	15	4	12	18
nRYr	26	16	5	11	10
rRYn	6	4	4	4	1
nRYy	8	3	3	5	9

[a] number of selected sequences cut by DNase I
[b] sites of drug inhibition of DNase I cutting
[c] sites of drug stimulation of DNase I cutting

different specificity patterns. A comparison of their effects on DNase I cutting is given in Table 1, where drug-induced inhibition or stimulation is reported for each base-pair arrangement.

We were able to analyze 323 base pairs and to identify 108 sites cleaved by DNase I alone. In the presence of MX, 44 sites are inhibited and 29 are enhanced to different extents, whereas the diaza derivative inhibited 68 sites and stimulated 42.

Hence, BBR 2894 exhibits a larger number of inhibition and stimulation sites, which points to the recognition of a larger variety of base arrangements. Interestingly, almost 90% (38 of 44) of all sequences that are protected by MX are also protected by BBR 2894. Therefore, the vast majority of MX binding sites are shared by the diaza derivative. In addition, the diaza derivative shows 30 new protection sites.

Two-base analysis. Table 1 seems to indicate that, in our DNA fragments, not all base doublets are cut by DNase I with the same efficiency. In particular, such sequences as CC, GG, GA, AA, and TA are poorly recognized by the enzyme. Hence, a modulation in the cutting frequencies induced by the drug at these sites cannot be safely analyzed. However, even from the simple two-base analysis, it is evident that the two drugs exhibit modified preferences. If anthraquinone inhibition effects are considered indicative of drug location along the DNA chain, it can be inferred that MX prefers alternating sites such as AC, GT, TG, GC, CG, whereas BBR 2894, in addition to alternating CA and CG, can be located at pyrimidine-pyrimidine sites such as TT, CT and TC, most of which are not recognized by the parent drug.

Triplet analysis. Because the location of the bound drug may not always coincide with the enzyme cutting site and the template occupancy by MX (and possibly BBR 2894) may span as many as 3 base pairs (3), a statistical examination has been extended to flanking bases as well. Considering 2 bases 5′ and two bases 3′ of the cutting site seems to be sufficient to give an overall consistent picture of the sequence preferences exhibited by the test drugs (Table 2). In fact, extending the examination to a larger number of flanking bases did not alter the specificity outcome to an appreciable extent (not shown).

The data are presented here in terms of purine (R) and pyrimidine (Y) triplet combinations. The marked difference in drug distribution emerging from Table 1 is still evident. In agreement with previous results (14–16), MX clearly recognizes alternating sequences. From the present analysis it is particularly effective with 5′-yRY-3′ (and the complementary 5′-RYr-3′), 5′-YRy-3′ and 5′-yYR-3′ (DNase I cuts occur between the bases in capital letters). Also, BBR 2894 seems to be effective on alternating sites; in this case, however, the most effective recognition occurs at sequences 5′-YRy-3′ (and the complementary 5′-rYR-3′) and 5′-yYR-3′. Moreover, the diaza derivative is able to interfere efficiently with 5′-yYY-3′, 5′-rYY-3′ and 5′-YYr-3′ triplets.

The efficiency in DNase I cleavage inhibition by the test drugs, considering individual base triplets (together with their complementary counterparts), is reported in Fig. 3. Because of the low occurrence of some of the sequences, only significant data are presented. These account for 24 of 32 possible triplet pairs.

The frequency of DNase I inhibition of MX suggests CTA, GCA, ACT, TAC, CAC and TTA (along with their complementary triplets) as the most significant. On the other hand, such sequences as ATC, TCA, TCC, and CTC (in general, TC-containing triplets) are very poorly affected, which should correspond accordingly to low affinity targets for MX. We fail to find (A/T)CA preferences (7 inhibitions of 20 sites) and cannot get reliable information about the under-represented (A/T)CG.

In the case of BBR 2894, there is a general increase of the frequency of inhibition and 13 sequences of 24 experience more than 75% protection of DNase I sites. This confirms the increase in the number of accepted triplets, which corresponds to less stringent requirements for drug binding to

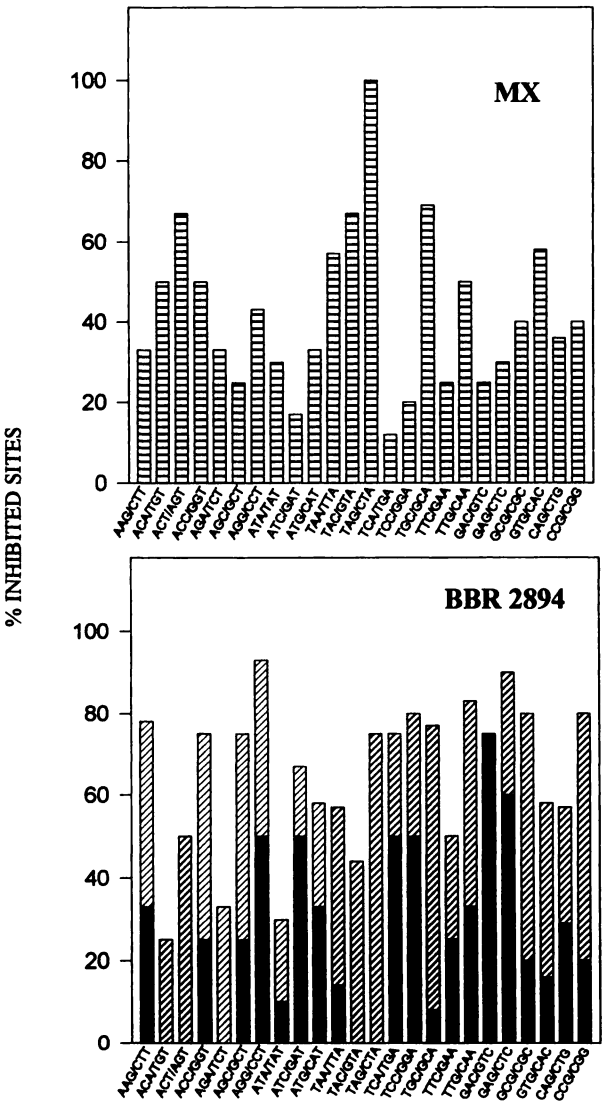

Fig. 3. Sequence specificity of DNase I cleavage inhibition induced by MX and BBR 2894. *Bottom*, contribution of "non-MX sites" (■) to total inhibition (▨). DNase I cutting occurs either between the first and the second base or between the second and third base.

DNA. As mentioned before, 38 of 68 BBR 2894 sites are in common with MX and share the same specificity requirements. The contribution to total inhibition arising from the remaining 30 "non-MX" sites is presented in Fig. 3 (*black bars*). The most relevant effects are at the level of YYY triplets, in particular YCT or CTY, and RYY triplets, the most distinctive being GTC, which is never found in the "MX-like" sites. On the other hand, low affinity sequences are characterized by two adenines located in the first and third positions.

Differential cleavage patterns. Representative differential cleavage patterns obtained from densitometric analysis are reported in Fig. 4. A comparison between BBR 2894 and MX shows that, on the average, the two drugs are characterized by a similar distribution of footprints along the DNA chain. The main difference is represented by a frequent 1 or 2 base-pair shift of the maximum stimulation or inhibition effect. Again, all MX suppression footprints are common to BBR 2894, which is further characterized by a number of new inhibition sites that occur in pyrimidine-rich regions. These facts confirm the data presented above.

Almost every protected sequence is associated with some enhancement of the cutting at nearby sites. As proposed in the literature, this is possibly attributable to both a mass action effect and a local deformation of DNA structure upon drug binding, which renders accessible sites more susceptible to enzyme cutting (35). Drug-enzyme and ternary drug-enzyme-DNA interactions could also play a role in increasing cutting efficiency.

Thermodynamics and Stereochemistry of DNA-Binding

Spectrophotometric titrations. To evaluate the thermodynamic and stereochemical effects of the carbon-to-nitrogen isosteric substitution on drug binding to DNA, the interaction between MX and BBR 2894 with DNA of known sequence was investigated using spectrophotometric techniques. In particular, the alternating polynucleotides poly(dA-dT) and poly(dG-dC) were examined. The results are reported in Table 3. Our data for MX are in very good agreement with literature reports of similar experimental conditions and confirm the drug preference for GC sites over AT sites (3). BBR 2894 binds to DNA with an affinity of at least 1 order of magnitude lower than that of MX at physiological conditions. This is consistent with the remarkably higher aza-anthraquinone concentration required to yield good footprinting data (Fig. 2). Like MX, BBR 2894 binds preferentially to GC sequences, albeit with a lower specificity ($K_{GC}/K_{AT} \cong 2$ for BBR 2894 and 4 for MX).

Chiroptical studies. DNA unwinding and linear dichroism experiments indicate that monoaza- and diaza-BBR derivatives are intercalating agents (30, 36). Induced circular dichroism is observed for the test compounds in the visible region in the presence of poly(dG-dC) and of poly(dA-dT) (Table 3). For BBR 2894, induced rotational strength is negative using both polynucleotides, whereas for MX it is positive and more intense. Hence, BBR 2894 and MX exhibit a substantially different orientation of the planar chromophore in the drug-DNA intercalation complex (37–39).

Discussion

The carbon-to-nitrogen isosteric substitution causes important changes in the recognition of DNA sequences by the anthracenedione derivatives. Not only is the strength of binding substantially altered but also the drug location along the nucleic acid is remarkably rearranged. The presence of two hydroxyl groups at positions 1 and 4 of the planar moiety in MX could also contribute to different sequence specificity, as recently reported (40). However, DNase I footprinting experiments with either MX or its 1,4-dehydroxyl congener, ametantrone, gave almost superimposable DNA cleavage patterns (not shown), which suggests that a minor role (if any) is played by —OH substitution in this context. This is in keeping with identical sequence preferences exhibited by MX and ametantrone in stimulating topoisomerase II-mediated DNA cleavage (41).

The DNase I footprinting experiments with MX confirm in part previous literature data, which indicated that 5′-pyrimidine-purine-3′ was a general binding preference (14, 16). However, we fail to find 5′-(A/T)CA and 5′-(A/T)CG as the principal consensus sequences, as suggested by a careful

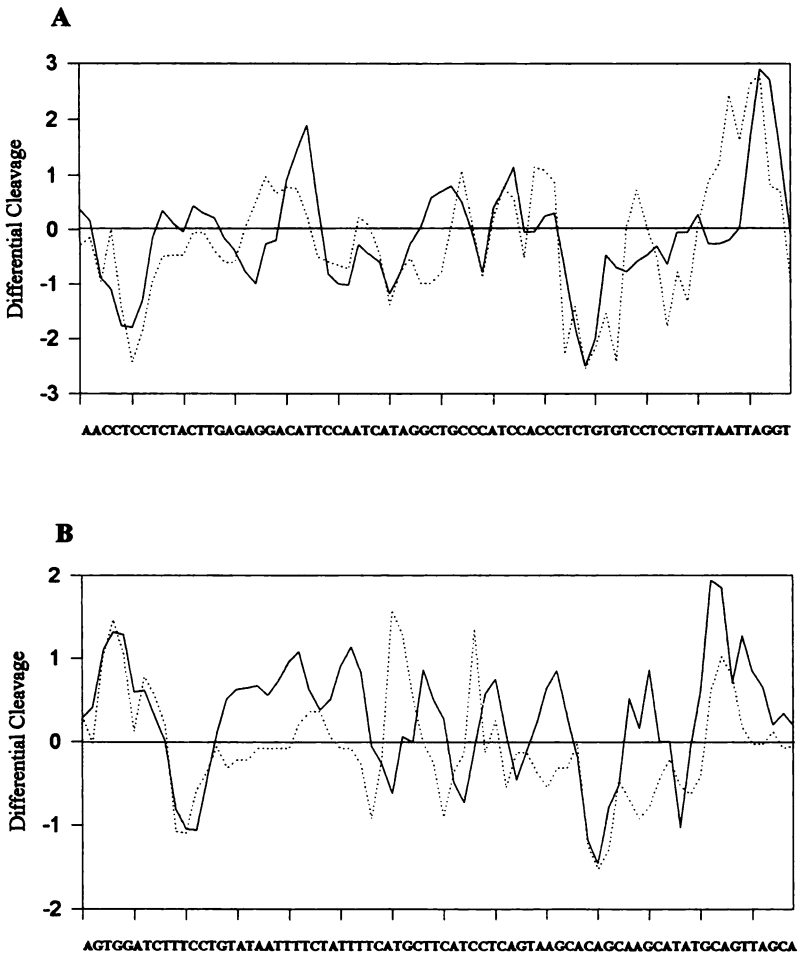

Fig. 4. Differential cleavage plots comparing the susceptibility to cutting by DNase I in the presence of 5 μM MX (*solid line*) or 10 μM BBR 2894 (*dotted line*). Negative values correspond to ligand-protected sites, positive values to enhanced cleavage. A, SV40 (*Bam*HI-*Acc*I restriction fragment). B, SV40 (*Taq*I-*Eco*RI restriction fragment).

TABLE 3
Effects of DNA sequence upon DNA-binding affinity and chiroptical properties in 0.15M EDTA/Tris/NaCl buffer, pH 7.0, 25°

DNA sequence	MX		BBR 2894	
	DNA-binding affinity	Induced circular dichroism[a] (molar ellipticity)	DNA-binding affinity	Induced circular dichroism[a] (molar ellipticity)
	$K_i \times 10^{-5}$ M^{-1}[b]		$K_i \times 10^{-5}$ M^{-1}[b]	
poly (dA-dT)	10.8 ± 1.1	+5,500	0.95 ± 0.4	−1,700
poly (dG-dC)	39.8 ± 2.6	+7,500	2.1 ± 0.5	−3,500

[a] In the drug absorption region.
[b] Intrinsic binding constant.

sequence analysis examining MX-induced transcriptional inhibition on the 497 base-pair fragment that contains the UV5 promoter (15). (A/T)CG-containing triplets were found to be cut only twice by DNase I in our experiments. In both instances, cutting was inhibited by MX. Hence, they could represent effective binding sites for the anthraquinone, although the number of observations is too small to draw any statistically relevant conclusion. Instead, the (A/T)CA triplet, cut significantly (20 times) by DNase I in the examined DNA fragments, is inhibited in 7 instances (35%) only. This seems to be an indication of poor rather than efficient recognition, especially when the above data is compared with the figures obtained for other sequences. On the other hand, triplets favored on the basis of the present footprinting analysis are found in six of the 14 sites of blocked transcripts induced by MX. Thus, a reasonably consistent picture of MX sequence preferences emerges from the comparison of data obtained using different experimental techniques and test conditions, which points to the reliability of the analytical methods described above.

An examination of most effective MX-binding sequences reveals that the base flanking the pyrimidine-purine intercalating pair is almost invariably a pyrimidine. Taking for granted that the planar portion of MX is inserted between two alternating bases (3, 16), the third base in the triplet should accommodate the hydroxyethylaminoethylamino side chain, which is believed to play an important role in recognizing the topoisomerase II-DNA cleavable complex. Interestingly, the sequence specificity for MX to induce topoisomerase II-mediated DNA cleavage is a pyrimidine located toward the 5′ end of the cutting site. Hence, recognition in the drug-DNA-enzyme complex seems to relate well to recognition of DNA alone by MX.

The specificity of BBR 2894 for DNA is less pronounced,

just as its binding affinity is lower. Interestingly, two sets of preferred binding sites are observed. The first, accounting for 57% of total inhibition, overlaps that found for MX almost perfectly. The second shows a new, unprecedented characteristic of the aza-anthraquinones: the preference for 5′-YCT, 5′-CTY, and 5′-RTC regions. Taking into account these extra sites will cause a more even distribution of the drug along DNA (Figs. 3 and 4). Our results imply also the ability of the drug to intercalate into DNA sequences that are not recognized by MX, which requires a higher flexibility of drug orientation into the base-pair pocket and, in any event, a modified binding geometry with reference to the parent anthraquinone. Indeed, as shown in Table 3, the sign of induced circular dichroism is reversed and the molar ellipticity is considerably altered when comparing DNA-bound MX with DNA-bound BBR 2894.

Similar observations apply to the monoaza-anthraquinones (not shown). Indeed, they also exhibit the two sets of DNA recognition sites, with the MX-like sites accounting for 70–85% of the total inhibition of DNase I cleavage. They also show a modified intercalation geometry and a reduced (intermediate) binding to DNA. The aza-anthraquinones lack the OH groups at position 1,4 of the tricyclic ring system. Along with a different stereochemistry of the intercalated complex, that fact may account, at least in part, for the loss of affinity for the nucleic acid. In addition, different contributions from the side-chain groups (MX contains two extra hydroxyls) may further affect thermodynamics of complex formation.

Finally, it is worth trying to correlate DNA-binding properties of the test drugs and their biological responses. In fact, DNA interaction is suggested to be a necessary component for mediating aza-anthracenedione-induced cell death, although it cannot fully account for differences in cytotoxic potential (36, 42).

Indeed, although MX acts mainly via interference with the topoisomerase II-DNA cleavable complex, BBR 2894 is unable to inhibit the enzyme but still preserves cytotoxic properties by generating a remarkable number (considerably larger than MX) of non-protein-associated DNA breaks (30).

Loss of stimulation of topoisomerase II mediated DNA cleavage cannot be attributed to lack of recognition of MX sites by BBR 2894, because the footprinting data show that this is not the case. Hence, the observed change in intercalation geometry must play a key role in impairing the appropriate drug-enzyme contacts. Indeed, proper interference with the enzyme-DNA complex requires a precise positioning of the drug pharmacophoric groups, so that a modified orientation of side-chains in BBR 2894 binding versus MX will markedly affect ternary complex formation. On the other hand, the wider distribution of BBR 2894 along DNA (and its less negative reduction potential) will increase its chance of damaging the nucleic acid via redox cycling and generation of hydroxy radicals, which do not require a precise stereochemistry of drug binding unless the toxic agent is close enough to its target. Here we witness a sort of compensation of two different toxicity mechanisms, generated by apparently minor chemical modifications of the anthraquinone structure.

References

1. Lown, J. W., ed. *Anthracycline and Anthracenedione-Based Anticancer Agents*. Elsevier, Amsterdam (1988).
2. Faulds, D., J. A. Balfour, P. Chrisp, and H. D. Langtry. Mitoxantrone, a review of its pharmacodynamic and pharmacokinetic properties, and therapeutic potential in the chemotherapy of cancer. *Drugs* **41**:400–449 (1991).
3. Lown, J. W., A. R. Morgan, S. F. Yen, Y. T. Wang, and W. D. Wilson. Characteristics of the binding of the anticancer agents mitoxantrone and ametantrone and related structures to deoxyribonucleic acids. *Biochemistry* **24**:4028–4035 (1985).
4. Minford, J., Y. Pommier, J. Filipski, K. W. Kohn, D. Kerrigan, M. Mattern, S. Michaels, R. Schwartz, and L. A. Zwelling. Isolation of intercalator-dependent protein-linked DNA strand cleavage activity from cell nuclei and identification as topoisomerase II. *Biochemistry* **25**:9–16 (1986).
5. Liu, L. F. DNA topoisomerase poisons as antitumor drugs. *Annu. Rev. Biochem.* **58**:351–375 (1989).
6. Tewey, K. M., G. L. Chen, E. M. Nelson, and L. F. Liu. Intercalative antitumor drugs interfere with the breakage-reunion reaction of mammalian DNA topoisomerase II. *J. Biol. Chem.* **259**:9182–9187 (1984).
7. Fisher, G. R., J. R. Brown, L. H. Patterson. Involvement of hydroxy radical formation and DNA strand breakage in the cytotoxicity of anthraquinone antitumor agents. *Free Radical Res. Commun.* **11**:117–125 (1990).
8. Kolodziejczyk, P., K. Reszka, J. W. Lown. Enzymatic oxidative activation and transformation of the antitumor agent mitoxantrone. *Free Radical Biol. Med.* **5**:13–25 (1988).
9. Capranico, G., P. De Isabella, S. Tinelli, M. Bigioni, and F. Zunino. Similar sequence specificity of Mitoxantrone and VM-26 stimulation of in vitro DNA cleavage by mammalian DNA topoisomerase II. *Biochemistry* **32**: 3038–3046 (1993).
10. Capranico, G., F. Zunino, K. W. Kohn, and Y. Pommier. Sequence-selective topoisomerase II inhibition by anthracycline derivatives in SV40 DNA: relationship with DNA binding affinity and cytotoxicity. *Biochemistry* **29**:562–569 (1990).
11. Capranico, G., M. Palumbo, S. Tinelli, M. Mabilia, A. Pozzan, and F. Zunino. Conformational drug determinants of the sequence specificity of drug-stimulated topoisomerase II DNA cleavage. *J. Mol. Biol.* **235**:1218–1230 (1994)
12. Palumbo, M., G. Capranico, S. Tinelli, M. Mabilia, A. Pozzan, and F. Zunino. Conformational properties of topoisomerase II inhibitors and sequence specificity of DNA cleavage. *J. Mol. Recognit.* **7**:227–231 (1994).
13. Kapuscinski, J., Z. Darzynkiewcz, F Traganos, and M. R. Melamed. Interaction of antitumor agents Ametantrone and Mitoxantrone (Novantrone) with double-stranded DNA. *Biochem. Pharmacol.* **30**:321–240 (1981).
14. Fox, K. R., M. J. Waring, J. R Brown, and S. Neidle. DNA sequence preferences for the anti-cancer drug mitoxanthrone and related anthraquinones revealed by DNase I footprinting. *FEBS Lett.* **202**:289–294 (1986).
15. Panousis, C., and D. R. Phillips. DNA sequence specificity of mitoxantrone. *Nucleic Acids Res.* **22**:1342–1345 (1994).
16. Chen, K-X., N. Gresh, and B. Pullman. A theoretical investigation on the sequence selective binding of mitoxantrone to double stranded tetranucleotide. *Nucleic Acids Res.* **14**:3799–3812 (1982).
17. Lown, J. W., and C. C Hanstock. High field ^{1}H-NMR analysis of the 1:1 intercalation complex of the antitumor agent mitoxantrone and the DNA duplex $[d(CpGpCpG)]_2$. *J. Biomol. Struct. Dyn.* **2**:1097–1106 (1985).
18. Kotovych, G., J. W. Lown, and J. P. K. Tong. High field ^{1}H and ^{31}P NMR studies on the binding of the anticancer agent mitoxantrone to $[d(CpGpCpG)]_2$. *J. Biomol. Struct. Dyn.* **4**:111–125 (1986).
19. Chaires, J. B., J. E. Herrera, and M. J. Waring. Preferential binding of Daunomycin to 5′(A/T)CG and 5′(AT)GC sequences revealed by footprinting titration experiments. *Biochemistry* **29**:6145–6153 (1990).
20. Pullman, B. Sequence specificity in the binding of antitumour anthracyclines to DNA: a success of theory. *Anti-Cancer Drug Des.* **7**:95–105 (1991).
21. Phillips, D. R., C. Cullinane, H. Trist, and R. J. White. *In vitro* transcription analysis of the sequence specificity of reversible and irreversible complexes of Adriamycin with DNA, in *Molecular Basis of Specificity in Nucleic Acid-Drug Interaction* (B. Pullman and J. Jortner, eds.). Kluwer Academic Press, Dordrecht, The Netherlands, 137–155 (1990).
22. Cheng, C. C., and R. K. Y. Zee-Cheng. The design, synthesis and development of a new class of potent antineoplastic anthraquinones. *Prog. Med. Chem.* **20**:83–118 (1983).
23. Murdock, K. C., R. G. Child, P. F. Fabio, R. B. Angier, R. E. Wallace, F. E. Durr, and R. V. Citarella. Antitumor agents: 1. 1,4-bis[(aminoalkyl)-amino]-9,10-anthracenediones. *J. Med. Chem.* **22**:1024–1030 (1979).
24. Krapcho, A. P., M. J. Maresch, M. P. Haker, L. Hazelhurst, E. Menta, A. Oliva, S. Spinelli, G. Beggiolin, C. Giuliani, G. Pezzoni, and S. Tognella. Anthracene-9,10-diones and aza bioisosteres as antitumor agents. *Curr. Med. Chem.* **2**:803–824 (1995).
25. Krapcho, A. P., M. E. Petry, Z. Getahum, J. J. Landi, J. Stallman, J. F. Polsenberg, C. E. Gallagher, M. J. Maresch, M. P. Haker, F. C. Giuliani, G. Beggiolin, G. Pezzoni, E. Menta, C. Manzotti, A. Oliva, S. Spinelli, and S. Tognella. 6,9-Bis[(aminoalkyl)amino]benzo[g] isoquinoline-5,10-diones: a novel class of chromophore-modified antitumor anthracenediones: synthesis and antitumor evaluations. *J. Med. Chem.* **37**:828–873 (1994).
26. Krapcho, A. P., M. J. Maresch, A. L. Helganson, K. E. Rosner, M. P. Haker, S. Spinelli, E. Menta, and A. Oliva. The synthesis of 6,9-bis[(aminoalkyl)-amino]substituted benzo[g] quinazoline and benzo[g]phalazine-5,10-diones via regiospecific displacements. *J. Heterocycl. Chem.* **30**:1597–1606 (1993).
27. Gandolfi, C. A., G. Beggiolin, E. Menta, M. Palumbo, C. Sissi, S. Spinelli, and F. Johnson. Chromophore-modified antitumor anthracenediones: syn-

thesis, DNA-binding and cytotoxic activity of 1,4-bis[(aminoalkyl)amino-]benzo[g]-phtalazine-5,10-diones. *J. Med. Chem.* **38**:526–536 (1995).
28. Krapcho, A. P., M. J. Maresch, C. E. Gallagher, M. P. Haker, E. Menta, A. Oliva, R. Di Domenico, G. Da Re, and S. Spinelli. Synthesis of 4-hydroxy-6,9-difluorobenzo[g]isoquinoline-5,10-diones and conversion to 4-hydroxy-6,9-bis[(aminoethyl)amino]benzo[g]isoquinoline-5,10-diones. *J. Heterocycl. Chem.* **32**:1963–1972 (1995).
29. De Isabella, P., M. Palumbo, C. Sissi, G. Capranico, N. Carenini, E. Menta, A. Oliva, S. Spinelli, A. P. Krapcho, F. C. Giuliani, and F. Zunino. Topoisomerase II DNA cleavage stimulation, DNA binding activity, cytotoxicity, and physico-chemical properties of 2-aza- and 2-aza-oxide-anthracenedione derivatives. *Mol. Pharmacol.* **30**:30–38 (1995).
30. De Isabella, P., M. Palumbo, C. Sissi, G. Capranico, E. Menta, A. Oliva, S. Spinelli, A. P. Krapcho, F. C. Giuliani, and F. Zunino. Physico-chemical properties, cytotoxic activity and topoisomerase II inhibition of 2,3-diaza-anthracenediones. *Biochem. Pharmacol.*, in press.
31. Bailly, C., A. W. Cuthbert, D. Gentle, M. R. Knowles, and M. J. Waring. Sequence-selective binding of Amiloride to DNA. *Biochemistry* **32**:2514–2524 (1993).
32. McGhee, J. D., and P. H. Von Hippel. Theoretical aspects of DNA-protein interactions: cooperative and non-cooperative binding of large ligands to a one-dimensional homogeneous lattice. *J. Mol. Biol.* **86**:469–489 (1974).
33. Bailly, C., and M. J. Waring. Comparison of different footprinting methodologies for detecting binding sites for a small ligand on DNA. *J. Biomol. Struct. Dyn.* **12**:869–898 (1995).
34. Denny, W. A., and L. P. G. Wakelin. Kinetics of the binding of Mitoxantrone, Ametantrone and analogues to DNA: relationship with binding mode and antitumor activity. *Anti-Cancer Drug Des.* **5**:189–200 (1990).
35. Goodisman, J., and J. C. Dabrowiak. Structural changes and enhancements in DNase I footprinting experiments. *Biochemistry*, **31**:1058–1064 (1992)
36. Hazelhurst, L. A., A. P. Krapcho, and M. P. Hacker. Correlation of DNA reactivity and cytotoxicity of a new class of anticancer agents: aza-anthracenediones. *Cancer Lett.* **91**:15–124 (1995).
37. Norden, B., and M. Kubista. Linear dichroism and induced circular dichroism for studying structure and interactions of DNA. *NATO ASI Ser. Ser. C. Math. Phys. Sci.* **242**:133–165 (1988).
38. Lyng, R., A. Rodger, and B. Norden. The CD of ligand-DNA systems. I. Poly(dG-dC) B-DNA. *Biopolymers* **31**:1709–1720 (1991).
39. Lyng, R., A. Rodger, and B. Norden. The CD of ligand-DNA systems. II. Poly(dA-dT) B-DNA. *Biopolymers* **32**:1201–1214 (1992).
40. Bailly, C., S. Routier, J. Bernier, and M. J. Waring. DNA recognition by two mitoxantrone analogues: influence of the hydroxyl groups. *FEBS Lett.* **379**:269–272 (1996)
41. De Isabella, P., G. Capranico, M. Palumbo, C. Sissi, A. P. Krapcho, and F. Zunino. Sequence selectivity of Topoisomerase II DNA cleavage stimulated by Mitoxantrone derivatives: relationships to drug DNA binding and cellular effects. *Mol. Pharmacol.* **43**:715–721 (1993).
42. Hazlehurst, L. A., A. P. Krapcho, and M. P. Hacker. Comparison of aza-anthracenedione-induced DNA damage and cytotoxicity in experimental tumor cell. *Biochem. Pharmacol.* **50**:1087–1094 (1995).

Send reprint requests to: Prof. Manlio Palumbo, Department of Pharmaceutical Sciences, University of Padova, Via Marzolo, 5–35131 Padova, Italy. E-mail: mpalumbo@purple.dsfarm.unipd.it